International Journal of Computer Engineering and Sciences Research

VOL. 04, NO. 02, March-April 2022
Pages 01–09 (ISSN: 2581-8481)
Available online at: www.ijcesr.com

Dissociative Excitation of the Even Doublet Levels of Cobalt Atom in e–$CoBr_2$ Collisions

Yu. M. Smirnov
National Research University “MPEI”, Krasnokazarmennaya str. 14, 111250, Moscow, Russia

***Abstract*.** Dissociative excitation of the even doublet levels of cobalt atom in e–$CoBr_2$ collisions was studied using the method of extended crossing electron and molecular beams. At an incident electron energy of 100 eV, dissociative excitation cross sections were measured for 57 radiative transitions from even doublet levels of the cobalt atom. Moreover, for six transitions from the $3d^7 4s(^3F^\circ)5s\ g\,^2F_{7/2}$ level, an optical excitation functions (OEF) were registered in the electron energy range E = 0–100 eV. The collision processes that make the main contribution to dissociative excitation in the near-threshold energy region are discussed.

Keywords –*electron-molecule collision; cross-section; dissociative excitation; radiative transition; energy level; optical excitation function*

I. Introduction

Excitation of the atom spectral lines in inelastic collisions of electrons with molecules (dissociative excitation) is still a poorly studied process. Under dissociative excitation, as a result of a single collision, molecule dissociates and appear free atoms, which are both in the ground and in excited states. This is followed by spontaneous radiative transitions of excited electrons of the atom and an atomic spectrum appears. This process takes part in the formation of multicomponent low-temperature plasma.

Dissociative excitation processes occur at higher energy than the excitation of atoms in electron-atom collisions since part of the energy of incident electrons is spent on breaking the bond between atoms in a molecule. In addition, some more of the electron energy can be spent on the excitation and/or ionization of the second atom, if the original molecule is diatomic, or molecular fragments in the case of triatomic and more complex molecules (when excited radicals are formed). Thus, the processes of dissociative excitation turn out to be much more complex than the excitation of atoms in electron-atom collisions, and as result, they are much less studied.

The fundamental review [1] discusses the growing role of mathematical modeling of various plasma devices and the need to obtain very extensive and reliable information about elementary processes occurring in plasma devices. In this case, the main attention of the authors of the review [1] is paid to the problems of the development of plasma installations and technologies used in the production of semiconductors and related industries. This determines the choice of molecules and elementary processes, as well as the range of particle energies that is relevant for these installations and technologies. The summary of data represented in [1, Table 1] provides information on CH_4, C_2H_4, C_2H_6, C_3H_8, SiH_4, Si_2H_6, GeH_4molecules, and, in addition, about 31 halogenated molecules. Data provided on *Elastic and Momentum Transfer Cross Sections, Rotational, Vibrational, and Electronic Excitations, Dissociation into Neutral Fragments,* and *Dissociative Electron Attachment*. All these processes are considered in the field of low energies. Ionization at an incident electron energy E = 5 keV considered separately for the total ionization cross sections in the case of CF_4 and C_3F_8 molecules; at E = 1 keV in the case of CF_4 molecules – the cross sections of dissociative ionization with the formation of CF_3^+, CF_2^+, CF^+, F^+, and C^+ ions.

As follows from the previous paragraph, dissociative ionization is the only process considered in [1] in the energy range from the threshold to E = 1–5 keV. However, in this energy range, the process of dissociative excitation is undoubtedly realized, in which atoms or ions detached from the initial molecule transit to excited states. Appearing in the volume of the plasma, excited atoms can affect its parameters for a number of reasons: a) the reactivity of excited atoms is much greater than that of atoms in the ground state; b) the spectrum of spontaneous emission of excited atoms can significantly affect the distribution of molecules and radicals by states, since for many atoms the most intense spectral lines are in the short-wavelength part of the spectrum (in vacuum ultraviolet with a wavelength of $\lambda \sim 100$ nm).

Although the processes of dissociative excitation occur at a higher energy of incident electrons than the processes of excitation of the same levels in electron-atom collisions, they can take place in modern devices such as gas lasers on metal halide vapors, in plasma-chemical etching reactors, as well as in various installations with beam plasma. It should be noted that lasers using molecules as an active medium in all cases have a significantly lower operating temperature than lasers with a discharge in pure metal vapors.

The bibliography of works on collisions for 1967–1973 [2] contains indications of 2356 publications (articles and reports at conferences) devoted to electron collisions, of which 196 are considered electron-molecular collisions (experiment). The titles of only 14 works contain the word "dissociative", but some authors do not use it, although the real content of the work is precisely dissociative excitement. However, the range of objects studied in the above 196 works is limited only to gases, mainly atmospheric, including water molecules.

In theoretical works, the same objects were mainly investigated as in experiments, with a small addition of HCl, H_2CO molecules. None of the 109 theoretical publications presented in [1] considers dissociative excitation. However, in subsequent years, the fundamental work [3] was published, in which the cross sections for dissociative excitation in collisions of electrons with homoatomic molecules H_2 and D_2 were calculated and some regularities in the behavior of the cross sections were established. Unfortunately, it remains unknown to what extent these regularities are valid for molecules that differ from the structure of the diatomic molecules studied in [3].

The study of dissociative collisions of electrons with molecules, the creation of beams of which requires an evaporation temperature much higher than room temperature, began only in 1991 with experiments with molecules of oxides BaO [4], LaO [5], YO [6]. At the same time, dissociative excitation in collisions of electrons with molecules of selenium [7] and [8], antimony [9] and tellurium [10] was investigated. In subsequent years, collisions of electrons with molecules of metal halides of I, II, III, and also partially VII and VIII groups were investigated.

Experiments with dihalides of Group VIII metals were continued using the method of extended crossing beams. In earlier works, dissociative excitation of even sextet states of the cobalt atom [11], dissociative excitation of $^2S°$-, $^2P°$- and $^2D°$ levels of the cobalt atom [12], as well as dissociative excitation of odd sextet levels of the cobalt atom [13] were studied in collisions of slow electrons with cobalt dibromide molecules. In this work, we studied the dissociative excitation of even doublet states of the cobalt atom in e–$CoBr_2$ collisions.

II. Main Experimental Conditions

The experiment was carried out by the method of extended crossing electron and molecular beams with registration of optical radiation of excited particles from the area of the beams intersection. A detailed discussion of the technique and methodology of this experiment is contained in recent papers [14], [15]. The evaporation of cobalt dibromide occurred as a result of heating the outer surface of a tantalum crucible with a test substance placed in it by an electron gun ray operating at an accelerating voltage of 10 kV. After preliminary heating at reduced power required for degassing the test substance (mainly to remove water molecules), the electron ray power was increased to the operating value, which provided the crucible temperature T = 1000 K, at which the concentration of $CoBr_2$ molecules in the region of intersection of the beams was $n = 6.8 \times 10^{10}$ cm^{-3}. The electron beam current density did not exceed 0.8 mA/cm^2 over the entire operating energy range of 0–100 eV, and a noticeable drop in the current density takes place only at energies less than 10 eV. The spectral resolution of the installation in the entire wavelength range studied in this work is ~ 0.1 nm.

In [3], using the example of H_2 and D_2 molecules, it was shown that the cross sections for dissociative excitation significantly depend on the vibrational level of the ground electronic state of the molecule prior to its collision with an electron. The most significant changes in the cross sections occur at small values of the vibrational quantum number v': for $v' = 0$ and 3, the cross-sections differ by more than a decimal order, while at $v' > 3$ the dependence $Q = f(v')$ becomes non-monotonic, and the range of possible values of the cross-sections are significantly narrowed. Therefore, it is most important to consider the behavior of the populations of precisely the low-lying vibrational levels.

The $CoBr_2$ molecule corresponds to the point symmetry group ($D_{\infty h}$) with the internuclear distance $r_{\mathrm{Co-Br}}$ = (2.32) Å [16]. Its optical properties are determined by three characteristic vibrations with fundamental frequencies $\nu_1 = (206)$ cm^{-1}, $\nu_2 = (40)$ cm^{-1}, $\nu_3 = 396 \pm 10$ cm^{-1}; the values in parentheses are obtained in [16] by an estimate. Obviously, at the above-mentioned temperature of evaporation of $CoBr_2$, the distribution of molecules over the levels of vibration ν_2 will be very wide due to the small value of the vibrational quantum. The estimate shows that the populations of two neighboring levels in the case of the vibration ν_2 differ by only 0.945 times, so that the level population with $v' = 10$ is 0.570 times of the level population with $v' = 0$. Such a broad distribution over vibrational levels in the region of small values of vibrational quantum number $v' = 0$–3 will change very little with temperature, whereas it is in this range of values that the v' partial cross sections of dissociative excitation most strongly depend on v' [3].

On the contrary, for the ν_3 vibration, the relative changes in the populations of the low-lying levels will be most significant. The estimated populations for ν_3 vibration are (in % of the total concentration of molecules in the beam): v' = 0 - 45.5, 1 - 25.8, 2 - 14.6, 3 - 8.3, 4 - 4.7, 5 - 2.65, 10 - 0.155. The ratio of the populations of two neighboring levels for this vibration is 0.567. With such a rapid decrease in populations, the total number of molecules in the beam at the lowest levels with $v' = 0 – 3$ is 94.2%, and it is the redistribution of molecules over these vibrational levels with temperature that most significantly affects the partial contribution of excitation from each of the initial levels to the resulting value of the cross section for dissociative excitation. It is necessary to take into account the presence of this factor when comparing experimental results with theoretical ones (when the latter appear).

III. Experimental results and their discussion

The spectrum of optical radiation arising from collisions of electrons with cobalt dibromide molecules was recorded in the wavelength range λ = 230–570 nm. In the visible part of the spectrum, in the same region, there are spectral bands of cobalt monobromide related to *A*, *B*, *C*, *D* systems (λ = 433–461 nm) [17] and *E*, *F*, *G*, *H*, *I* systems (λ = 467–560 nm) [18]. However, under the conditions of the present experiment, neither the spectral bands of CoBr, nor the spectral lines of the CoII ion were detected. This work presents the results related to the dissociative excitation of even doublet levels of the cobalt atom. At the energy of exciting electrons E = 100 eV, 57 cross sections were measured (including 9 blends); in the electron energy range E = 0–100 eV, the optical

Table 1. Cross-Sections for Dissociative Excitation of Cobalt Atom (with OEF recorded)

λ, nm	Lower level	J_{low}–J_{up}	E_{low}, cm^{-1}	Q_{100}, 10^{-18} cm^2	Q_{max}, 10^{-18} cm^2
474.611	$3d^7(^4F)4s4p(^3P^\circ)\ z^2G^\circ$	9/2–7/2	31699	0.18	0.19
478.507	$3d^7(^4F)4s4p(^3P^\circ)\ z^2F^\circ$	7/2–7/2	31871	0.50	0.53
492.500	$3d^8(^3F)4p\ y^4G^\circ$	9/2–7/2	32464	0.33	0.35
510.311	$3d^8(^3F)4p\ y^4G^\circ$	7/2–7/2	33173	0.41	0.44
517.348	$3d^8(^3F)4p\ y^2G^\circ$	9/2–7/2	33439	0.125	0.135
531.265	$3d^8(^3F)4p\ y^4F^\circ$	5/2–7/2	33945	0.37	0.39

Table 1. Columns 1-6 – the same as in table 2. Since these six transitions occur from the same upper level $3d^74s(^3F)5s\ g^2F_{7/2}$, related characteristics are not included in the table 1: E_{up} = 52763 cm^{-1}, Q_{max} – the cross section in the OEF maximum, $E(Q_{max})$= 90 eV – OEF peak position.

excitation function (OEF) was recorded for six transitions occurring from the $3d^74s(^3F)5s\ g^2F_{7/2}$ (E = 52763 cm^{-1}) level. For transitions from other levels, a sufficiently reliable registration of the OEF turned out to be impossible, since for them the excitation cross sections are small and almost all $Q_{100}<10^{-18}$ cm^2. The results obtained with the addition of the necessary spectroscopic information are presented in table. 1 (for transitions from $3d^74s(^3F)5s\ g^2F_{7/2}$ level) and in table. 2 (for transitions from other even doublet levels, with the exception of $3d^8(^3F)5s\ e^2F_{7/2,5/2}$).

At energies of exciting electrons of several tens of eV, dissociative excitation can occur through several competing channels, and this is reflected in the complex OEF structure shown in Fig. 1. In the region of low electron energies, the following channels for the excited cobalt atoms formation can be indicated (in parentheses after the channel equations are given the values of the threshold energy, eV, corresponding to the excitation of the λ = 535.350 nm line, the most intense line for which OEF was recorded):

$\mathrm{CoBr_2 + e \rightarrow Co^* + Br_2 + e'}$ (11.19), (1)

$\rightarrow \mathrm{Co^* + 2Br + e'}$ (13.16),

(2)

$\rightarrow \mathrm{Co^* + Br_2^* + e'}$ (~ 13.4),

(3)

$\rightarrow \mathrm{Co^* + Br^* + Br + e'}$ (~ 21.1),

(4)

$\rightarrow \mathrm{Co^* + Br_2^+ + e' + e''}$ (21.75),

(5)

$\rightarrow \mathrm{Co^* + Br^+ + Br + e' + e''}$ (25.00).

(6)

Here e and e′ are incident and scattered electrons, respectively; e″ is an electron knocked out of bromine atom or bromine molecule during their ionization. Asterisks mark particles in excited states. Reference data on the bond breaking energies were taken from [19]. The appearance potential E_{ap} = 13.0 ± 0.3 eV, measured by the OEF, agrees with the calculated for the reaction channel (2), i.e., the situation when an excited cobalt atom, as well as

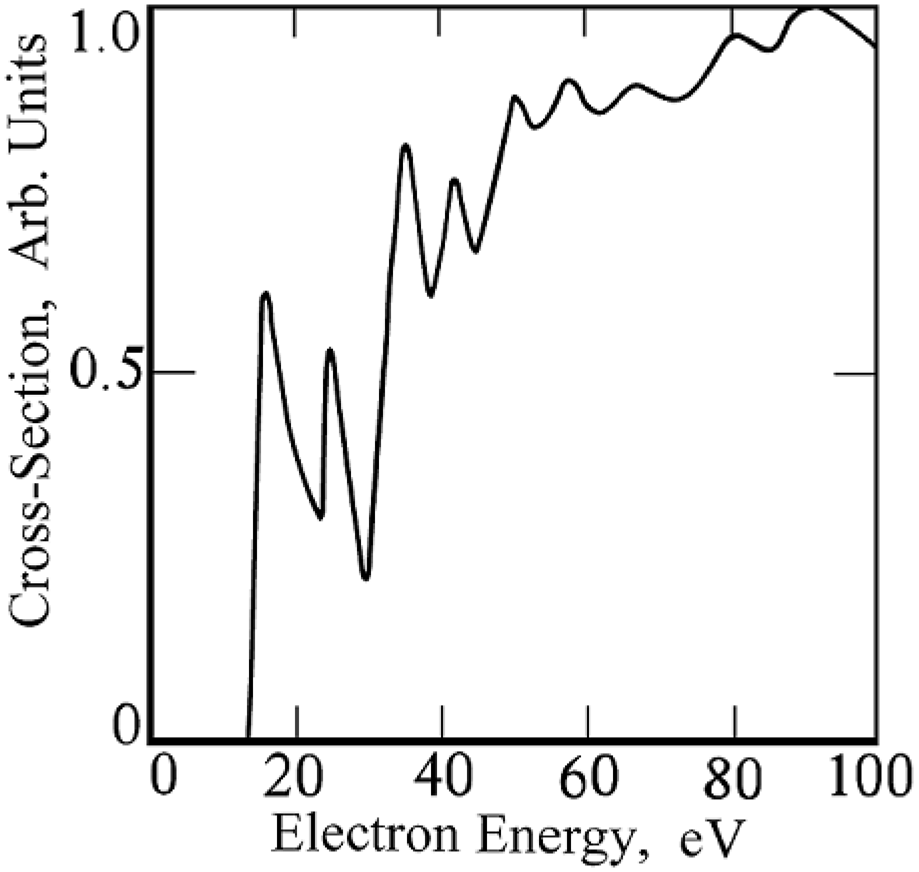

Fig. 1. The format of figure 1 is usual for representation of molecular OEFs: the scale on the abscissa axis is linear, on the ordinate axis is also linear. The curve is normalized to one at the maximum.

two free bromine atoms, which are in ground state, appears in a single collision of an electron with a molecule. For reaction channels (3) and (4), the exact values of E_{ap} have not been established, since it is not known in which excited states an atom or a bromine molecule are found to be as a result of the dissociation of a $CoBr_2$ molecule; moreover, if channels (3) or (4) are realized, the bromine atom or molecule is not in the only excited state, like the cobalt atom. Having reached at E = 15.5 ±0.5 eV the local maximum with a magnitude of 60% of the value at the main maximum, the OEF begins a rapid decline, which is succeeded by a repeated increase at E = 23 ± 1 eV, associated with the contribution of the channel (5). Some shift in the apparent onset of the OEF re-growth towards higher energies occurs due to the fact that the onset of the contribution of process (5) takes place in the rapidly decreasing section of the OEF associated with process (2). The further behavior of OEF is extremely difficult to interpret both due to an increase in the number of processes that are possible in this energy region, and due to the lack of information about the behavior in this energy region of processes that have already manifested themselves in the region of lower energies. Separating the contributions of numerous processes that are possible for incident electron energies above 30–50 eV seems to be an extremely difficult task for experiment, but, possibly, more realistic for theoretical consideration.

Analyzing the results presented in table. 2, it should first of all be noted that the explanation of both the numerical values of the cross sections for dissociative excitation and the dependence of the cross sections on the energy of incident electrons can hardly be based on the results of [3] due to the significant difference in the characteristics of the $CoBr_2$ molecule from the characteristics of the H_2 and D_2 molecules, studied in [3]. Therefore, we will restrict the discussion to only consideration of secondary processes (i.e., spontaneous radiative transitions) that occur after the population of the energy levels of the cobalt atom as a result of dissociative excitation.

The ground level of the cobalt atom $3d^74s^2\ a^4F_{9/2}$ is an even quartet, as are the seven higher levels nearest to it: three levels of the ground term $3d^74s^2\ a^4F$ and four levels of the $3d^8(^3F°)4s\ b^4F$ term. All higher levels up to E = 23207 cm^{-1} are also even (doublets or quartets). Among the odd levels, the sextets with the lowest energy related to $3d^7(^4F)4s4p(^3P°)\ z^6F°$, $3d^7(^4F)4s4p(^3P°)\ z^6D°$, $3d^7(^4F)4s4p(^3P°)\ z^6G°$ terms, located in the energy range E = 23611–26597 cm^{-1}. The lowest energy (about 32000 cm^{-1}) among the odd doublet levels have those related to the $3d^7(^4F)4s4p(^3P°)\ z^2G°$ and $3d^7(^4F)4s4p(^3P°)\ z^2F°$ terms. Thus, completely allowed transitions from even doublet terms studied in this work can occur only to the two above $z^2G°$ and $z^2F°$ terms, as well as to the $y^2F°$, $y^2G°$, $z^2D°$, $z^2S°$, $z^2H°$ terms, having higher energy. Due to this structure of energy levels, the allowed transitions of the cobalt atom in the short-wavelength part of the spectrum are limited by the wavelength λ = 474.611 nm, and in the long-wavelength part, by the wavelength λ = 760.635 nm. Lines that are outside this range, provided by forbidden transitions, violating the rules of selection or by ΔL, or by multiplicity.

The results, that are presented in the table 2, are clearly reflected in the partial state diagram of the cobalt atom. In this case, in the diagram, as well as in the table 2, are not shown $3d^8(^3F°)5s\ e^2F_{7/2,5/2}$ (E = 45924 and 46745 cm^{-1}) levels – the lowest of the group of high-lying even doublets; all allowed transitions from this pair of levels are in the yellow-red part of the spectrum outside the range recorded in this work. It should also be noted that among the forbidden transitions registered by us, presented in Table 2, transitions to sextet levels are completely absent, although such transitions are known from the data of a number of spectroscopic publications. However, in the important work [20], which we used in the preparation of Table 1 and 2, there are transitions to sextet levels from the $3d^74s(^5F°)5s\ f^4F$ quartet, but not from the doublets. It is possible that the intensities of the radiative doublet → sextet transitions are too low under the conditions of our experiment.

It should be noted that the forbidden transitions in Table 2 are provided not only by the above-mentioned violations of the selection rules for ΔL or by multiplicity, but for a large number of lines also by two-electron transitions. As you can see in the Table 2, almost all of the upper levels presented in it refer to the $3d^8(^3F°)4d$ configuration. The only exception is the $3d^74s(^3F°)5s\ g^2F$ term, from the levels of which transitions occur to the levels of $3d^8(^3F°)4p$ and $3d^7(^4F)4s4p(^3P°)$ configurations. The transition to the levels of the second of these configurations is provided by the completely allowed transformation $5s \rightarrow 4p$, while the first is provided by the forbidden two-electron transformation $4s5s \rightarrow 3d4p$. Transitions from the remaining even doublets take place to odd levels of the same two configurations, however, transitions to $3d^8(^3F°)4p$ ($4d \rightarrow 4p$) are allowed in this case, and the two-electron transitions to $3d^7(^4F)4s4p(^3P°)$ ($3d4d \rightarrow 4s4p$) are forbidden. In this case, without taking into account blends, only three values of the cross sections Q_{100} exceed 10^{-18} cm^2, while all the others are in the range of 10^{-18}–10^{-19} cm^2.

Table 2. Dissociative excitation cross-sections of the cobalt atom (without OEFs recorded)

λ, nm	Transition	J_{low}–J_{up}	E_{low}, cm^{-1}	E_{up}, cm^{-1}	Q_{100}, 10^{-18} cm^2	Q_{50}, 10^{-18} cm^2	Q_m/Q_a	Q_m/Q_a (aver.)
1	2	3	4	5	CoBr$_2$	CoI	8	9
470.416	$3d^74s4p\ z^4D°–3d^84d\ e^2P$	5/2–3/2	29948	**51200**	0.12	0.029	4.14	3.79
539.047	$3d^84p\ y^4D°–3d^84d\ e^2P$	5/2–3/2	32654	51200	0.15	0.041	3.66	
563.612	$3d^74s4p\ z^2D°–3d^84d\ e^2P$	5/2–3/2	33462	51200	0.16	0.045	3.56	
486.209	$3d^74s4p\ z^2F°–3d^84d\ e^2D$	5/2–3/2	32781	**53343**	0,17	0.057	2.98	2.93
522.128	$3d^84p\ y^4F°–3d^84d\ e^2D$	3/2–3/2	34196	53343	0.15	0.049	3.06	
526.424	$3d^74s4p\ z^2D°–3d^84d\ e^2D$	3/2–3/2	34352	53343	0.20	0.073	2.76	
430.103	$3d^74s4p\ z^4F°–3d^84d\ e^2D$	5/2–5/2	29216	**52460**	0.08	0.023	3.48	3.33
454.079	$3d^74s4p\ z^4D°–3d^84d\ e^2D$	3/2–5/2	30443	52460	0.10	0.031	3.22	
485.563	$3d^74s4p\ z^2F°–3d^84d\ e^2D$	7/2–5/2	31871	52460	0.11	0.032	3.44	
517.738 {	$3d^84p\ y^4D°–3d^84d\ e^2D$ $3d^74s4p\ z^2D°–3d^84d\ e^4G$	3/2–5/2 5/2–5/2	33150 33462	52460 52772	} 0.20	0.070	2.86	

518.306	$3d^74s4p\ z^2F^\circ$–$3d^84d\ g^4F$	5/2–5/2	32781	52069	0.28	0.11	2.55	
518.346	$3d^84p\ y^4F^\circ$–$3d^84d\ e^2D$	7/2–5/2	33173	52460				
526.245	$3d^74s4p\ z^2D^\circ$–$3d^84d\ e^2D$	5/2–5/2	33462	52460	0.15	0.049	3.07	
532.171	$3d^84p\ y^4G^\circ$–$3d^84d\ e^2D$	5/2–5/2	33674	52460	0.30	0.086	3.49	
539.976	$3d^84p\ y^4F^\circ$–$3d^84d\ e^2D$	5/2–5/2	33945	52460	0.18	0.055	3.27	
494.859	$3d^84p\ y^4D^\circ$–$3d^84d\ e^2G$	5/2–7/2	32654	**52856**	0.12	0.043	2.79	2.78
496.790	$3d^74s4p\ z^2G^\circ$–$3d^84d\ e^2G$	7/2–7/2	32733	52856	0.19	0.070	2.72	
497.994	$3d^74s4p\ z^2F^\circ$–$3d^84d\ e^2G$	5/2–7/2	32781	52856	0.35	0.13	2.69	
515.484	$3d^74s4p\ z^2D^\circ$–$3d^84d\ e^2G$	5/2–7/2	33462	52856	0.11	0.035	3.14	
521.169	$3d^84p\ y^4G^\circ$–$3d^84d\ e^2G$	5/2–7/2	33674	52856	0.38	0.15	2.53	
521.182	$3d^74s4p\ z^2F^\circ$–$3d^84d\ e^4D$	7/2–7/2	31871	51052				
533.952	$3d^84p\ y^2G^\circ$–$3d^84d\ e^2G$	7/2–7/2	34133	52856	0.46	0.18	2.55	
427.611	$3d^74s4p\ z^4F^\circ$–$3d^84d\ e^2G$	7/2–9/2	28777	**52156**	0.16	0.048	3.33	3.20
488.699	$3d^74s4p\ z^2G^\circ$–$3d^84d\ e^2G$	9/2–9/2	31699	52156	0.14	0.040	3.50	
496.659	$3d^84p\ y^4D^\circ$–$3d^84d\ e^2G$	7/2–9/2	32027	52156	1.15	0.32	3.60	
	$3d^84s\ b^4F$–$3d^74s4p\ z^6F^\circ$	9/2–11/2	3482	23611				
507.687	$3d^84p\ y^4G^\circ$–$3d^84d\ e^2G$	9/2–9/2	32464	52156	0.09	0.031	2.90	
507.741	$3d^74s4p\ z^2F^\circ$–$3d^84d\ e^4D$	7/2–5/2	31871	51560				
534.133	$3d^84p\ y^2G^\circ$–$3d^84d\ e^2G$	9/2–9/2	33439	52156	1.28	0.41	3.13	
534.909	$3d^84p\ y^4G^\circ$–$3d^84d\ e^2G$	7/2–9/2	33466	52156	0.61	0.20	3.05	
554.697	$3d^84p\ y^2G^\circ$–$3d^84d\ e^2G$	7/2–9/2	34133	52156	0.18	0.066	2.73	
417.763	$3d^74s4p\ z^4G^\circ$–$3d^84d\ e^2H$	11/2–9/2	28845	**52775**	0.10	0.037	2.71	3.01
498.785	$3d^84s\ b^4F$–$3d^74s4p\ z^6F^\circ$	5/2–5/2	4690	24733	2.29	0.16	14.3	
498.803	$3d^74s4p\ z^2G^\circ$–$3d^84d\ e^2H$	7/2–9/2	32733	52775				
510.007	$3d^84p\ y^4F^\circ$–$3d^84d\ e^2H$	7/2–9/2	33173	52775	0.14	0.042	3.33	
536.278	$3d^84p\ y^2G^\circ$–$3d^84d\ e^2H$	7/2–9/2	34133	52775	2.62	0.25	10.5	
489.718	$3d^84p\ y^2G^\circ$–$3d^84d\ e^2H$	9/2–11/2	31699	**52113**	0.33	0.087	3.79	5.82
508.786	$3d^84p\ y^4G^\circ$–$3d^84d\ e^2H$	9/2–11/2	32464	52113	0.21	0.048	4.37	
535.350	$3d^84p\ y^2G^\circ$–$3d^84d\ e^2H$	9/2–11/2	33439	52113	3.59	0.39	9.20	
473.777	$3d^84s\ b^4P$–$3d^84p\ y^2D^\circ$	3/2–3/2	15774	36875	0.46	0.13	3.54	
473.813	$3d^74s4p\ z^2F^\circ$–$3d^84d\ f^2F$	7/2–5/2	31871	52970				
512.473	$3d^74s4p\ z^2D^\circ$–$3d^84d\ f^2F$	5/2–5/2	33462	52970	0.37	0.11	3.36	
512.480	$3d^84p\ y^4D^\circ$–$3d^84d\ e^4G$	5/2–7/2	32654	52161				
530.721	$3d^84p\ y^2G^\circ$–$3d^84d\ f^2F$	7/2–5/2	34133	**52970**	0.16	0.040	4.00	4.00
536.959	$3d^74s^2\ a^4P$–$3d^84p\ y^4D^\circ$	3/2–5/2	14036	32654	3.36	0.35	9.60	
	$3d^74s4p\ z^2D^\circ$–$3d^84d\ f^2F$	3/2–5/2	34352	52970				
1	2	3	4	5	CoBr$_2$	CoI	8	9
428.738	$3d^74s4p\ z^4F^\circ$–$3d^84d\ f^2F$	7/2–7/2	28777	**52094**	0.15	0.037	4.05	4.03
451.418	$3d^74s4p\ z^4D^\circ$–$3d^84d\ f^2F$	5/2–7/2	29948	52094	0.20	0.050	4.00	
498.179	$3d^74s4p\ z^2F^\circ$–$3d^84d\ f^2F$	7/2–7/2	32027	52094	0.15	0.034	4.41	
514.247	$3d^84p\ y^4D^\circ$–$3d^84d\ f^2F$	5/2–7/2	32654	52094	0.21	0.056	3.75	
528.348	$3d^84p\ y^4F^\circ$–$3d^84d\ f^2F$	7/2–7/2	33173	52094	0.67	0.16	4.18	
536.673	$3d^84p\ y^4G^\circ$–$3d^84d\ f^2F$	7/2–7/2	33466	52094	0.22	0.061	3.71	
417.089	$3d^74s4p\ z^4G^\circ$–$3d^74s5s\ g^2F$	7/2–5/2	29735	**53704**	0.18	0.052	3.46	4.34
429.793	$3d^74s4p\ z^4D^\circ$–$3d^74s5s\ g^2F$	3/2–5/2	30443	53704	0.11	0.028	3.93	
476.714	$3d^74s4p\ z^2G^\circ$–$3d^74s5s\ g^2F$	7/2–5/2	32733	53704	0.34	0.075	4.47	
477.823	$3d^74s4p\ z^2F^\circ$–$3d^74s5s\ g^2F$	5/2–5/2	32781	53704	0.41	0.086	4.77	
486.938	$3d^84p\ y^4F^\circ$–$3d^74s5s\ g^2F$	7/2–5/2	33173	53704	0.18	0.038	4.74	
516.606	$3d^74s4p\ z^2D^\circ$–$3d^74s5s\ g^2F$	3/2–5/2	34352	53704	0.21	0.045	4.66	
424.558	$3d^74s4p\ z^4F^\circ$–$3d^74s5s\ g^2F$	5/2–7/2	29216	**52763**	0.13	0.031	4.19	4.59
474.611	$3d^74s4p\ z^2G^\circ$–$3d^74s5s\ g^2F$	9/2–7/2	31699	52763	0.27	0.060	4.50	
478.507	$3d^74s4p\ z^2F^\circ$–$3d^74s5s\ g^2F$	7/2–7/2	31871	52763	0.25	0.056	4.46	
492.500	$3d^84p\ y^4G^\circ$–$3d^74s5s\ g^2F$	9/2–7/2	32464	52763	0.11	0.025	4.41	
517.348	$3d^84p\ y^2G^\circ$–$3d^74s5s\ g^2F$	9/2–7/2	33439	52763	0.13	0.030	4.34	

517.969	$3d^74s4p\ z^2D°–3d^74s5s\ g^2F$	5/2–7/2	33462	52763	0.26	0.11	2.36
518.019	$3d^74s4p\ z^2F°–3d^84d\ g^4F$	7/2–9/2	31871	51170			
523.708	$3d^84p\ y^4G°–3d^74s5s\ g^2F$	5/2–7/2	32674	52763	0.30	0.067	4.47
531.265	$3d^84p\ y^4F°–3d^74s5s\ g^2F$	5/2–7/2	33945	52763	0.92	0.16	5.75

Table 2. Reference spectroscopic data are given according to [20]: wavelength λ, transition, internal quantum number of the lower J_{low} and upper J_{up} levels, energy of the lower E_{low} and the upper E_{up} levels, Q_{100} is the excitation cross section in e–CoBr$_2$ collisions at the incident electron energy E = 100 eV, Q_{50} is the excitation cross section in e–Co collisions at the incident electron energy E = 50 eV, Q_m/Q_a is the ratio of the cross sections $Q_{100}(\text{CoBr}_2)/Q_{50}(\text{Co})$, Q_m/Q_a(aver.) is the average value of the cross sections ratio for the energy levels in bold.

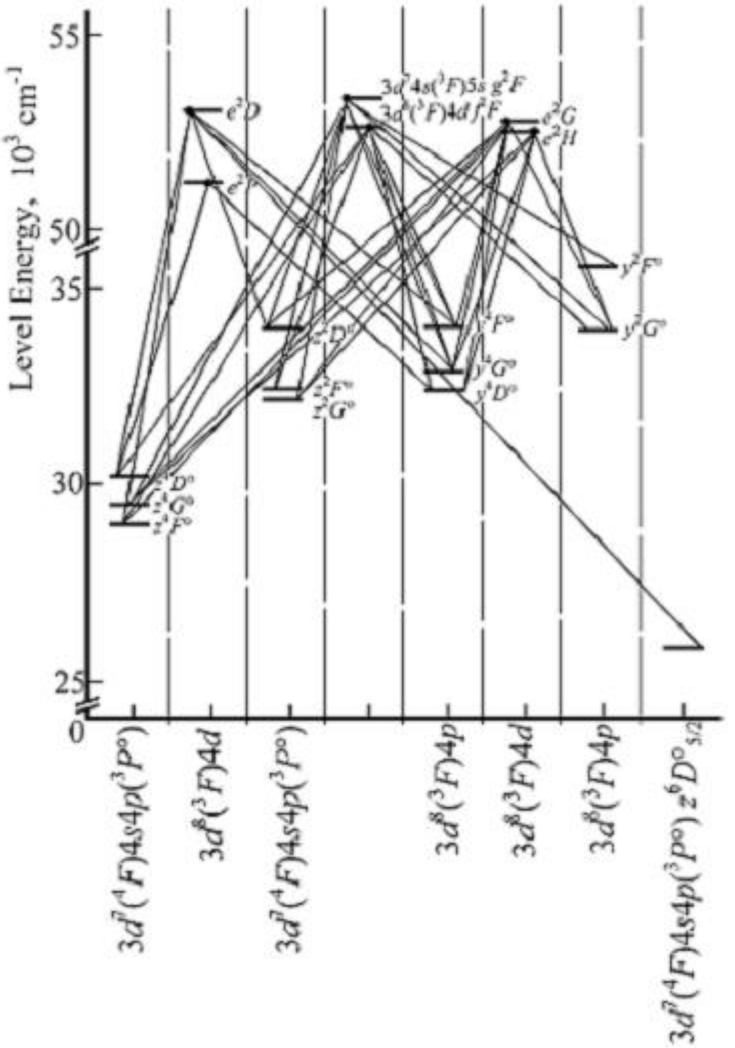

Fig. 2. Partial diagram of even doublet levels of the cobalt atom with spontaneous transitions investigated. As far as possibly, labels denoting states have been placed below the abscissa axis. This applies first of all to configuration labels. When several terms exist for the same configuration, term symbols are placed within the plot area. States that differ in parity are separated by dashed vertical lines. The terms represented levels are shown without splitting by J.

The results of this work can be compared with the cross sections for the excitation of a cobalt atom in e–Co collisions, which were obtained by the author of this work within the framework of a program for the systematic study of electron–atom and electron–molecular collisions. The Q_m/Q_a column shows the ratio of

$Q_{100}(CoBr_2)$ to $Q_{50}(Co)$, and the Q_m/Q_a(aver.) column shows the average values of this ratio for the levels, highlighted in bold in column 5. The calculation does not take into account the contribution of blends and lines with double classification. As can be seen in these columns, for all the studied transitions, the values of $Q_{100}(CoBr_2)$ are several times higher than $Q_{50}(Co)$. The same correlation of the cross sections in electron–molecular and electron–atom collisions was obtained in previous studies (for example, [12]). It should be kept in mind that in the case of electron–atom collisions, the cross section at $E = 100$ eV is smaller than at $E = 50$ eV: specifically for the 535.350 nm line, $Q_{100}(Co)/Q_{50}(Co) = 0.77$ (the value obtained according to the recorded OEF in the study of e–Co collisions).

IV. Conclusion

Plasma devices, in which vapors of molecular substances act as a working medium, are becoming more and more widespread. These include gas lasers based on metal halide vapors, plasma-chemical reactors designed for plasma-chemical etching, coating, obtaining semiconductor films and layered structures with special properties, etc. implementation of which requires extensive information about elementary processes occurring in multicomponent low-temperature plasma [1]. Dissociative excitation is one of the least studied among these processes. The above-said work is aimed at partially filling the gap in this area.

References

[1] W.M. Huo and Y.-K. Kim, *IEEE Transactions on Plasma Science*, 27 (1999) 1225.
[2] Physics of the Electronic and Atomic Collisions, Bibliography 1967–1973, Issue 2, Pt. 1, Edited by E.S. Solov’ev, Nauka, Leningrad, 1977. (in Rus.)
[3] R. Celiberto, U.T. Lamanna and M. Capitelli, *Physical Review A*,50 (1994) 4778.
[4] A.N. Kuchenev, Yu.M. Smirnov, *Chemical Physics*, 10 (1991) 1462.
[5] Yu.M. Smirnov, *J. Appl. Spectrosc*., 55 (1991) 1263. DOI: 0021-9037/91/5506-1263.
[6] A.N. Kuchenev, Yu.M. Smirnov, *High Energy Chemistry*, 25 (1991) 202. (in Rus.)
[7] Yu.M. Smirnov, *J. Appl. Spectrosc*., 55 (1991) 315. (in Rus.)
[8] Yu.M. Smirnov, *High Temperature*, 44 (2006) 656.
[9] Yu.M. Smirnov, *High Energy Chemistry*, 26 (1992) 7. (in Rus.)
[10] Yu.M. Smirnov, *High Energy Chemistry*, 26 (1992) 99. (in Rus.)
[11] Yu.M. Smirnov, *Russian J. Phys. Chem. B: Focus on Physics*, 8 (2014) 761. DOI: 10.1134/S1990793114110086.
[12] Yu.M. Smirnov, *Russian J. Phys. Chem. B: Focus on Physics*, 10 (2016) 876. DOI: 10.1134/S1990793116060270.
[13] Yu.M. Smirnov, *Russian J. Phys. Chem. B: Focus on Physics*, 14 (2020) 209. DOI: 10.1134/S1990793120020293.
[14] Yu.M. Smirnov, *J. Phys. B: At. Mol. Opt. Phys.*,48 (2015) 165204 (11 pp). DOI: 10.1088/0953-4075/48/16/165204.
[15] Yu.M. Smirnov, *J. Phys. B: At. Mol. Opt. Phys*.,49(2016)175204 (11 pp). DOI: 10.1088/0953-4075/49/17/175204.
[16] Molecular Constants of Inorganic Combinations, Reference Book, Edited by K.S. Krasnov, Chimiya, Leningrad, 1979. (in Rus.)
[17] S.V.K. Rao, P.T. Rao, *Indian J. Phys*., 36 (1962) 609.
[18] N.V.K. Rao, Y.P. Reddy, P.T. Rao, *Indian J. Pure & Appl. Phys*., 10 (1972) 389.
[19] L.V. Gurvich, G.V. Karachevtsev, V.N. Kondrat’ev, et.al., Energies of the Chemical Bindings Rupture. Ionization Potentials and Affinity for Electron, Nauka, Moscow, 1974. (in Rus.)
[20] J.C. Pickering and A.P. Thorne, *Astrophys. J. Suppl. Ser*., 107 (1996) 761.